Preparation and Characterization of Nitrogen and Oxygen Containing Graphite-like Pyropolymers from 5-(2-Pyridyl)-2,4-pentadiyn-1-ol

Min Chul Suh and Sang Chul Shim*

Department of Chemistry, Korea Advanced Institute of Science and Technology, 373-1 Kusung-Dong, Yusung-Gu, Taejon 305-701, Korea

Received May 17, 1996. Revised Manuscript Received October 30, 1996[⊗]

5-(2-Pyridyl)-2,4-pentadiyn-1-ol was polymerized over $NbCl_5$- or $TaCl_5$-based catalysts followed by pyrolysis to obtain graphite-like pyropolymers. The black metathesis polymer, poly[5-(2-pyridyl)-2,4-pentadiyn-1-ol], has the structure of a fully conjugated backbone and was converted into a polyacene-based polymer having pyridyl pendant groups. The pyropolymers prepared by vacuum pyrolysis over 700 °C have nitrogen atoms incorporated into graphene sheets. The polymers were characterized by elemental analysis, TGA, FT-IR, laser Raman, NMR, XPS, X-ray diffraction, temperature-programmed desorption experiments, charge/discharge experiments, and SEM and TEM studies.

Introduction

Graphite is a very important and interesting material in the lithium battery application. However, there have been a lot of efforts to obtain better carbon materials for use as an anode of lithium ion electrochemical cells which will ultimately affect the energy density and performance of such batteries. Recently, Dahn et al. obtained very high capacity materials from hard carbons made by pyrolyzing organic polymers at temperatures near 1000 °C (theoretical specific capacity of graphite: 372 mAh/g).[1,2] The hard carbon prepared at low temperature has properties similar to those of polyacene-based polymers prepared under 1000 °C. The structure of precursor polymers is very important for the preparation of graphite-like structures with different electrochemical properties. We have studied polyacene-based polymers or graphite-like pyropolymers from various precursor polymers to investigate their applicability as electrode materials. Investigation of the microstructure of each graphene sheet as well as the macrostructure of the pyropolymers can be helpful to clarify the Li insertion mechanism into the graphite-like material.[3]

There have been many studies on metathesis polymerization of various substituted acetylenes by transition-metal catalysts. A number of catalysts based on groups 5 and 6 transition metals (Nb, Ta, Mo, W, etc.) have been exploited to polymerize substituted acetylenes, especially sterically crowded ones.[4,5] In our previous work, we reported $NbCl_5$- or $TaCl_5$-based catalyst systems to be very effective for selective 1,2-polymerization of asymmetrically substituted diacetylenes and enynes,[6−11] and these polymers were pyrolyzed to give high capacity graphite-like pyropolymers for Li insertion/deinsertion reactions as shown in Scheme 1.

Scheme 1

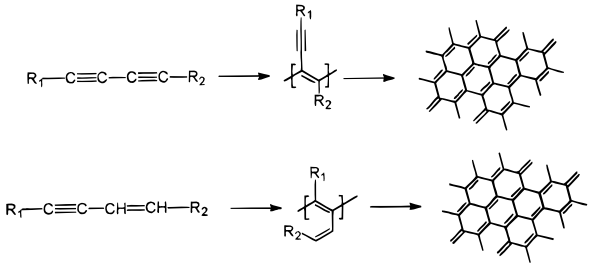

The precursor polymers showed different carbonization yields according to their substituents. The pendant group has the important role of supressing the evaporation of the polymer itself. The morphology of final pyropolymers is also different in accordance with the substituents attached to the starting polymers.[11] Precursor polymers having nitrogen atoms and hydroxyl groups gave higher carbonization yields even though the pyrolysis pathway is very difficult to predict due to incorporation of the heteroatom into the graphene sheets. Dahn et al. prepared nitrogen-containing carbons in various ways.[12] They suggested that there is "chemical nitrogen" which reacts irreversibly with lithium, making these materials not useful as anodes for Li-ion cells.

In this article, we report the polymerization and pyrolysis of 5-(2-pyridyl)-2,4-pentadiyn-1-ol (PyPDO) to investigate the effect of heteroatom and heteroaromatic

[⊗] Abstract published in *Advance ACS Abstracts,* December 15, 1996.

(1) Zheng, T.; Liu, Y.; Fuller, E. W.; Tseng, S.; Sacken, U.; Dahn, J. R. *J. Electrochem. Soc.* **1995**, *142*, 2581.
(2) Xue, J. S.; Dahn, J. R. *J. Electrochem. Soc.* **1995**, *142*, 3668.
(3) Yata, S.; Osaki, T.; Hato, Y.; Takehara, N.; Kinishita, H.; Tanaka, K.; Yamabe, T. *Synth. Met.* **1990**, *38*, 177.
(4) Masuda, T.; Takahashi, T.; Higashimura, T. *Macromolecules* **1985**, *18*, 311.
(5) Masuda, T.; Higashimura, T. *Acc. Chem. Res.* **1984**, *17*, 51.
(6) Lee, H. J.; Shim, S. C. *J. Chem. Soc., Chem. Commun.* **1993**, 1420.
(7) Lee, H. J.; Shim, S. C. *J. Polym. Sci., Part A: Polym. Chem.* **1994**, *32*, 2437.
(8) Lee, H. J.; Suh, M. C.; Shim, S. C. *Synth. Met.* **1995**, *71*, 1763.
(9) Lee, H. J.; Suh, M. C.; Shim, S. C. *Synth. Met.* **1995**, *73*, 141.
(10) Suh, M. C.; Shim, S. C. *Macromolecules* **1995**, *28*, 8707.
(11) Shim, S. C.; Suh, M. C.; Kim, D. S. *J. Polym. Sci., Part A: Polym. Chem.* **1996**, *34*, 3131.
(12) Weydanz, W. Z.; Way, B. M.; van Buuren, T.; Dahn, J. R. *J. Electrochem. Soc.* **1994**, *141*, 900.

S0897-4756(96)00283-9 CCC: $14.00

ring in the pendant group on the structure of resulting polymers.

Experimental Section

Instruments. Proton and ^{13}C NMR spectra were recorded on Bruker AM-300 and Bruker AM-200 spectrometers with chemical shifts being referenced against TMS as an internal standard or the signal of the solvent $CDCl_3$. ^{13}C NMR CP/MAS spectra were carried out on the Varian UNITYplus (75 MHz). Mass spectra were determined at 70 eV with a Hewlett-Packard 5985A GC/MS interface by the electron impact (EI) method. Elemental analyses (EA) were performed on the elemental analyzer of Foss Heraeus Analysentechnik instrument. FT-IR spectra were recorded on a Bomem MB-100 spectrophotometer. Laser Raman spectra were obtained using 514 nm line of an argon ion laser with a back scattering geometry by a laser Raman microscope (Jobin-Yvon Ramanor U-1000). Thermogravimetric analyses (TGA) were performed under the nitrogen atmosphere at a heating rate of 20 °C/min with a Perkin-Elmer TGA7. The X-ray photoelectron spectroscopy (XPS) was carried out using ESCALAB MK II of VG Scientific Co. The X-ray diffractogram was measured by a Rigaku D/MAX-RC 12 kW X-ray diffractometer using Ni-filtered Cu Kα radiation at a scan speed of 4°/min. The position of the diffraction peaks was calibrated by the peaks of Si powder as a standard. Temperature-programmed desorption experiments were carried out using on-line Micromass (Varian) quadrupole mass spectrometer as a detector and an interfaced computer for data recording. Scanning electron microscopy (SEM) was measured by a Phillips 535M. Transmission electron microscopy (TEM) was carried out with a JEOL JEM2000EX operating at 200 kV.

Materials. 2-Bromopyridine, 2-methyl-3-butyn-2-ol, bis(triphenylphosphine)palladium(II) chloride, copper(I) iodide, ethylamine, $TaCl_5$, and other organometallics as cocatalysts were obtained commercially from Aldrich Chemical Co. and used without further purification. $NbCl_5$ was purified by sublimation prior to use. 2-Ethynylpyridine was prepared by the reported method.[13] Solvents were purified by standard methods,[14] care being taken to remove moisture as completely as possible for the polymerization solvent (chlorobenzene). Solvents of reagent grade were used for chromatography without further purification. A chromatography column of silica gel was prepared with Kieselgel 60 (70−230 mesh).

Synthesis of 5-(2-Pyridyl)-2,4-pentadiyn-1-ol (PyPDO). *2-Methyl-4-(2-pyridyl)-3-butyn-2-ol.* 2-Methyl-3-butyn-2-ol (4.85 mL, 50 mmol) was added to a solution of bis(triphenylphosphine)palladium(II) chloride (420 mg, 0.6 mmol), copper(I) iodide (114 mg, 0.6 mmol), and 2-bromopyridine (2.86 mL, 30 mmol) in triethylamine (100 mL) under nitrogen atmosphere. The mixture was heated to 40 °C and maintained at that temperature for 1 h. After evaporation of solvents, the reaction mixture was extracted with ether and separated by column chromatography on a silica gel column using *n*-hexane/ethyl acetate (1/1, v/v) as an eluent to obtain 2-methyl-4-(2-pyridyl)-3-butyn-2-ol in 98% yield (Scheme 1). ^1H NMR ($CDCl_3$, 300 MHz) δ 8.51 (d, 1H), 7.58 (m, 1H), 7.35 (d, 1H), 7.17 (m, 1H), 3.78 (s, 1H), 1.61 (s, 6H) ppm; ^{13}C NMR ($CDCl_3$, 75 MHz) δ 150.0, 143.1, 135.9, 126.1, 122.0, 94.9, 80.7, 64.7, 31.1 ppm.

2-Ethynylpyridine. The mixture of 2-methyl-4-(2-pyridyl)-3-butyn-2-ol (4.185 g, 25.96 mmol) and sodium hydroxide (2.5 g, 62.5 mmol) in benzene (100 mL) was refluxed for several hours. The mixture was filtered through a silica gel column eluting with *n*-hexane/diethyl ether (1/1, v/v) and the solvent was removed under reduced pressure to give 2-ethynylpyridine in 80% yield. ^1H NMR ($CDCl_3$, 300 MHz) δ 8.49 (d, 1H), 7.57 (m, 1H), 7.38 (d, 1H), 7.17 (m, 1H), 3.10 (s, 1H) ppm; ^{13}C NMR ($CDCl_3$, 75 MHz) δ 149.8, 142.1, 136.0, 127.3, 123.2, 82.5, 77.0 ppm.

(13) Suh, M. C.; Kim, S. N.; Lee, H. J.; Shim, S. C.; Suh, I.-H.; Lee, J.-H.; Park, J.-R. *Synth. Met.* **1995**, *72*, 51.

(14) Perrin, D. D.; Armarego, W. L. F. *Purification of Laboratory Chemicals*; Pergamon Press: Oxford, U.K., 1988.

Scheme 2

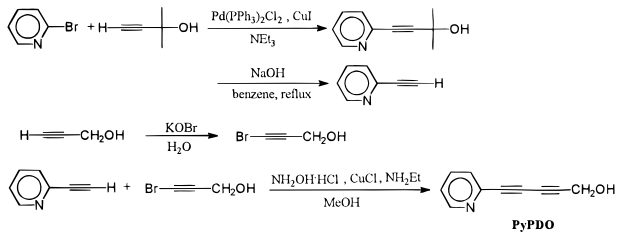

Table 1. Polymerization of PyPDO[a]

no.	catalyst	$[M]_0$, M	[cat.], mM	[cocat.], mM	polymer yield (%)[b]
1	$NbCl_5$·(*n*-Bu)$_4$Sn	0.5	16.7	16.7	68
2	$TaCl_5$·(*n*-Bu)$_4$Sn	0.5	16.7	16.7	97
3	$TaCl_5$·Et_3SiH	0.5	10	10	80
4	$MoCl_5$·(*n*-Bu)$_4$Sn	0.5	16.7	16.7	trace

[a] Polymerized in chlorobenzene at 115 °C for 24 h. [b] The precipitated polymers in methanol were gravimetrically estimated.

3-Bromo-2-propyn-1-ol. 3-Bromo-2-propyn-1-ol was obtained in 90% yield as a viscous liquid from propargyl alcohol by the same method used for 5-bromo-4-pentyn-1-ol. ^1H NMR ($CDCl_3$, 300 MHz) δ 4.26 (s, 2H), 2.15 (s, 1H) ppm; ^{13}C NMR ($CDCl_3$, 75 MHz) δ 78.1, 51.6, 45.7 ppm.

PyPDO. PyPDO was prepared by the Chodkiewicz and Cadiot coupling of 2-ethynylpyridine and 3-bromo-2-propyn-1-ol in 70% yield (Scheme 2), mp 114−116 °C. ^1H NMR ($CDCl_3$, 200 MHz) δ 8.53 (d, 1H), 7.65 (t, 1H), 7.47 (d, 1H), 7.28 (d, 1H), 4.42 (s, 2H) 3.55 (s, 1H) ppm; ^{13}C NMR ($CDCl_3$, 75 MHz) δ 149.9, 141.8, 136.5, 128.4, 123.7, 82.7, 76.3, 73.8, 69.3, 51.1 ppm; MS (70 eV) *m/e* 157 (M^+, 27.2), 128 (M^+ − CHO, 100).

Polymerization. All the procedures for the preparation of the catalyst system and polymerization reaction were carried out under a dry argon atmosphere. A typical procedure is as follows (Table 1, second row): A mixture of TaCl, (186 mg, 0.52 mmol) and PyPDO (2.45 g, 15.6 mmol) was weighed in Ar atmosphere and added to fully degassed chlorobenzene. A 0.1 M solution of (*n*-Bu)$_4$Sn in chlorobenzene (5.20 mL, 0.52 mmol) was added with continuous stirring at 80 °C for 15 min. When the solution turned black, the solution was heated to 115 °C and stirred for 24 h. Methanol was added to the reaction mixture followed by suction filtration to obtain poly(PyPDO). The product was purified by Soxhlet extraction with methanol for 12 h to remove residual $TaCl_5$ completely and dried overnight under vacuum at 50 °C (polymer yield 2.23 g, 97%).

Vacuum Pyrolysis. The reaction of poly(PyPDO) under vacuum was carried out using a Cole-Parmer programmable vacuum furnace. The specimen (about 1 g) was introduced into a SUS-exmet (stainless steel expanded metal) reactor (inside diameter, 25 mm; height, 500 mm). After the cell was closed, it was placed in a vacuum furnace and evacuated to around 10^{-1} Torr by an oil pump. The specimens were dried for 10 min at 50 °C and the reactor was heated at a ramping rate of 10 °C/min. After reaction under vacuum, the pyroproduct was cooled to room temperature, the vacuum was released, and the product was removed from the reactor. The reaction at the highest temperature is controlled for exactly 30 min. The pyropolymers are denoted by poly(PyPDO)-T_p (T_p: pyrolysis temperature).

Temperature-Programmed Desorption (TPD) Experiment. A sample of 3.4 mg of poly(PyPDO) was introduced into a NMR cell (diameter: 10 mm) which has a ground-glass high-vacuum stopcock and fritted filter disk prior to sealing by flame. The cell was subsequently evacuated at high vacuum ($\sim 6 \times 10^{-4}$ Torr). Each TPD experiment was started at room temperature and was stopped at 800 °C using a programmable tube furnace at a heating rate of 6.2 °C/min.

Charge/Discharge Experiments. The working electrodes used in the electrochemical tests are fabricated by mixing poly(PyPDO)-800 powder with 7 wt % of poly(tetrafluoroethylene)

Scheme 3

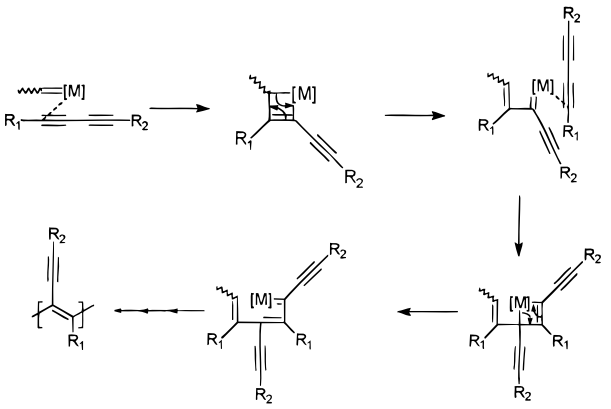

binder. The resulting slurry is deposited on SUS-exmet (stainless steel expanded metal) and pressed to form a thin pellet with a thickness of 200−300 μm. It was dried under vacuum for 12 h at 150 °C. Lithium metal is used as a counter and a reference electrode. The charge (deinsertion)/discharge (insertion) cycling tests for poly(PyPDO)-800 were carried out using computer-controlled constant-current cyclers between 0 and 2.5 V at a constant current density of 24.8 mA/g.

Results and Discussion

The average molecular weight of poly(PyPDO) could not be determined due to its insolubility in any organic solvent. The black poly(PyPDO) was obtained in the highest yield with the [PyPDO]/[$TaCl_5$]/[(n-Bu)$_4$Sn] = 30/1/1 system as shown in Table 1.

In our previous report, we have shown that enynes have a low reactivity because of the competing polymerization between double bonds and triple bonds. Termination started when the number of repeating units reaches approximately 10−15 on metathesis.[10] The reactivity is not much higher when the monomers are diacetylene derivatives, the average molecular weight being not more than several thousand. Nevertheless, some diacetylene monomers can be polymerized to give an insoluble powder. The poly(2,4-hexadiyn-1,6-diol) (PHDO)[7] and poly(PyPDO) are insoluble in organic solvents. In the polymerization of diacetylene derivatives, the steric hindrance directly affects the reactivity of the two acetylene moieties. When one of the two acetylene moieties having sterically less hindered substituents (R_1) participates in the polymerization, the reactivity of the remaining acetylene moiety is decreased and the metathesis polymerization of the diacetylene derivatives can result in specific 1,2-polymerization. A plausible reaction pathway is shown in Scheme 3.

Because pyropolymers from poly(PyPDO) as well as poly(PyPDO) itself are insoluble in any organic solvent, it is very difficult to obtain information about the structure of the intermediate since only the solid-state techniques can be utilized.

All the heat-treated pyropolymers were subjected to elemental analysis (EA). The molar ratios of hydrogen to carbon and nitrogen to carbon decreased as the pyrolysis temperature was raised as shown in Table 2. The degree of carbonization can be controlled by T_p applied, since the H/C and N/C molar ratios vary with the pyrolysis temperature (T_p). We can also predict a likely structure of the pyropolymers from these results even though the exact structure cannot be obtained due

Table 2. Pyrolysis of Poly(PyPDO)[a]

	weight percent				
material[b]	C	H	N	[H]/[C][c]	[N]/[C][c]
poly(PyPDO)[d]	67.8	4.5	7.8	0.79	0.10
poly(PyPDO)-250	71.5	3.5	8.4	0.58	0.10
poly(PyPDO)-400	60.2	2.3	7.3	0.45	0.10
poly(PyPDO)-500	64.9	2.2	7.4	0.40	0.10
poly(PyPDO)-600	72.3	1.8	6.7	0.29	0.08
poly(PyPDO)-700	78.2	1.4	6.5	0.22	0.07
poly(PyPDO)-800	80.8	1.2	5.5	0.18	0.06

[a] Pyrolyzed in vacuo (~10^{-1} Torr) for 30 min. [b] The number after poly(PyPDO) denotes the heat-treatment temperature (T_p). [c] The molar ratios of hydrogen to carbon and nitrogen to carbon were determined by EA. [d] Polymerized in chlorobenzene at 115 °C for 24 h; $[M]_0$ = 0.5 M, [cat.] = [cocat.] = 16.7 mM.

Scheme 4

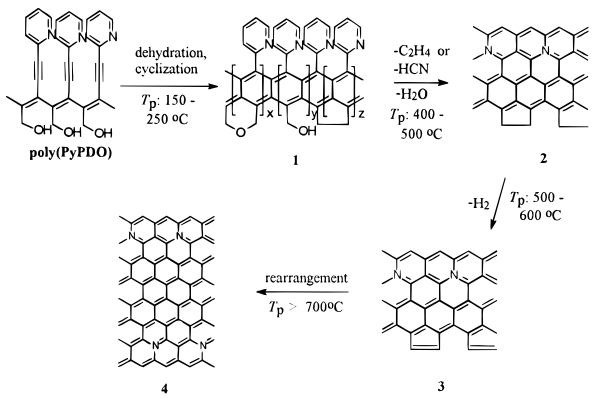

to the defect sites of the pyropolymers which are expected to show different [H]/[C] and [N]/[C] ratios. The outline of these synthetic routes is suggested as shown in Scheme 4.

According to Scheme 4, the triple bonds in the side chain of poly(PyPDO) cyclized to a polyacene-based structure with pyridyl pendant group (**1**) upon heat treatment accompanying dehydration from the hydroxymethyl pendant groups. At 250 °C, dehydration is not complete according to the ^{13}C NMR (CP/MAS) spectrum. Because the polymer easily traps moisture, the [H]/[C] ratio is somewhat larger than the theoretical value ([H]/[C] = 0.70). This can also be verified by TGA analysis.

We used various analytical techniques to elucidate the structure of polymers (**1**−**4**). The structure of **2** can be obtained by the condensation reaction of the carbon residue after ethylene or hydrogen cyanide is cleaved from the pyridyl rings of the pyropolymer [poly(PyPDO)-250], as shown in Scheme 4.

Because dehydration occurs in the range 150−250 °C, oxidation can occur from the micropores of the polymers by water vapor. Boehm reported that the possible structures of the surface oxygen groups are carboxyl groups, carboxylic anhydrides, lactone groups, lactols, hydroxyl groups, carbonyl groups, quinone-like groups, ether-type oxygen, etc.[15] Oxidation processes may also be involved in the pyrolytic pathway of poly(PyPDO) since dehydration can release water vapor into the micropores of these materials. The most probable oxygen functionalities, however, are ether-type oxygen in this case. The existence of oxygen is detected by EA and XPS (or ESCA) studies. The quantitative measure-

(15) Boehm, H. P. *Carbon* **1994**, *32*, 759.

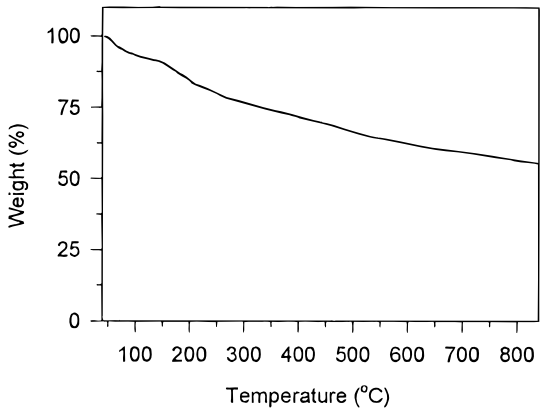

Figure 1. TGA of poly(PyPDO) (heating rate: 20 °C, N_2 atmosphere).

ment of oxygen content, however, is very difficult because of the easy adsorption of molecular oxygen or water vapor into these micropores. Oxygen contamination is a serious problem, especially on the surface. There is a large discrepancy between EA and XPS data. For example, the [O]/[C] of poly(PyPDO)-800 is only 0.04 in EA compared with 0.08 in the XPS analysis supporting the fact that molecular oxygen or water vapor in air can be easily readsorbed into the micropores of these specimens, especially on the surface. In other words, oxygen exists in poly(PyPDO)-T_p (T_p > 400 °C) not as a major component but as a contaminant on the surface. Incorporation of nitrogen functionalities as well as oxygen groups into the graphene layers is also very important in the application to Li ion batteries. Stanczyk et al. reported that nitrogen evolution is more difficult when the nitrogen atom is a component of the rings compared to the side-chain nitrogen functionalities such as amino aromatic or cyano aromatic precursors.[16] For poly(PyPDO)-700 and -800, the most probable nitrogen functionalities are quaternary nitrogens, and the electrochemical data are somewhat different from those of Dahn's materials.[12]

Figure 1 shows TGA of poly(PyPDO) indicating only 40% weight loss when T_p is raised near 840 °C. A lower pyrolysis temperature is required to obtain the same effect under vacuum, in general. The 6% weight loss in the region of 40−120 °C may correspond to the evaporation of H_2O trapped in the hydroxymethyl pendant groups of poly(PyPDO). Because of this moisture absorbed in the hydroxymethyl pendant groups of poly(PyPDO), the FT-IR spectrum of poly(PyPDO) shows very broad peak in the range 3200−3500 cm^{-1} as shown in Figure 2b. The 11.3% weight loss between 120 and 300 °C corresponds to the dehydration of pendant hydroxyl groups.

Significant information about the structures of poly(PyPDO) and heat-treated poly(PyPDO) at various temperatures was obtained from the FT-IR spectra as shown in Figure 2. The following vibrations are of particular importance: The stretching vibration of the triple bond in the monomer is observed near 2252 and 2227 cm^{-1} (Figure 2a). When this monomer is polymerized in fully degassed chlorobenzene solution by metathesis, only a single band at 2199 cm^{-1} is observed as shown in Figure 2b, indicating that only one of the

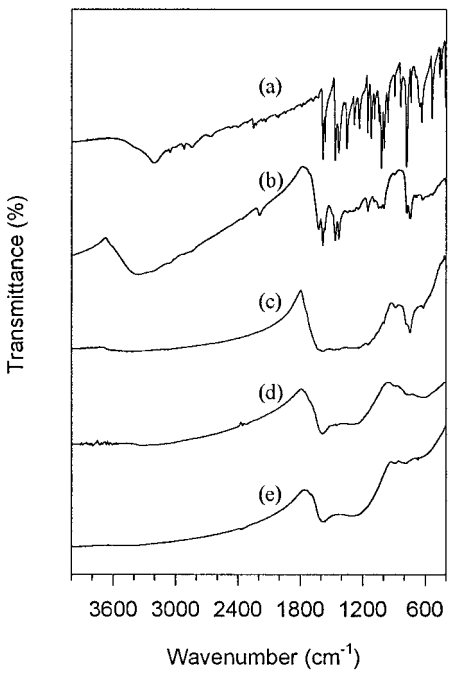

Figure 2. FT-IR spectra of (a) PyPDO (monomer), (b) poly(PyPDO), (c) poly(PyPDO)-250, (d) poly(PyPDO)-400, and (e) poly(PyPDO)-500.

two triple bonds is involved in polymerization. In the spectrum of PyPDO, very complex vibrational patterns are observed due to the pyridyl substituent. Generally, interaction between the ring C═C and C═N stretching vibrations result in two strong-to-medium intensity absorption bands about 100 cm^{-1} apart. In PyPDO, these absorptions are observed at 1584, 1561, 1464, and 1430 cm^{-1}, respectively. Bands of variable intensity are observed in the region 1300−1180 cm^{-1} due to in-plane deformation vibrations. The absorption of 780−740 cm^{-1} corresponds to typical C−H out-of-plane deformation vibration of 2-monosubstituted pyridines.[17] All of these bands are simplified upon polymerization as shown in Figure 2b. The O−H stretching bands near 3200 cm^{-1} and the C−O stretching band near 1020 cm^{-1} become broader and weaker upon polymerization (Figure 2a,b). The important absorption of polyconjugated polymers is detected near 1610 cm^{-1}. This band is due to the C═C stretching vibration of conjugated double bonds along polymer main and side chains. When the polymer was heat-treated at 250 °C for 30 min under vacuum, the stretching vibration of −OH and C≡C completely disappeared (Figure 2c) supporting the dehydration and cyclization of the pendant groups. When the temperature was raised to 400 °C, the out-of-plane C−H deformation band of the pyridyl ring is almost eliminated, as shown in Figure 2d. Since all the characteristic bands are lost when the pyrolysis temperature was raised over 500 °C (Figure 2e), the laser Raman method is utilized to characterize the pyropolymers. Figure 3 shows changes in the laser Raman spectra of poly(PyPDO) on heat treatment at various temperatures. All the pyropolymers reacted at T_p (600, 700, and 800 °C) exhibit broad peaks at around 1350 and 1630 cm^{-1}, indicating these products to have

(16) Stanczyk, K.; Dziembaj, R.; Piwoarska, Z.; Witkowski, S. *Carbon* **1995**, *33*, 1383.

(17) Socrates, G. *Infrared Characteristic Group Frequencies*; John Wiley & Sons: New York, 1980.

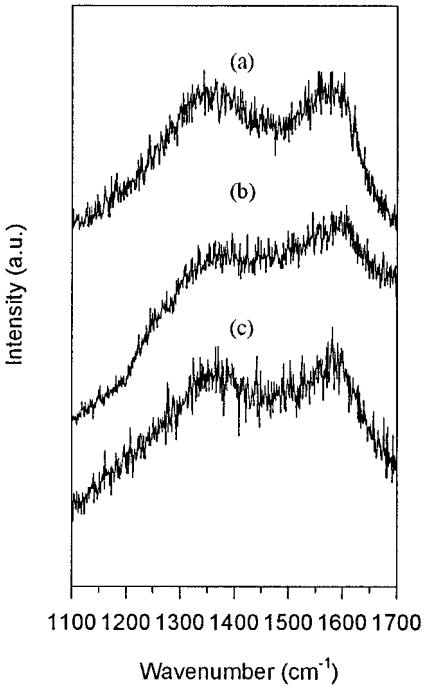

Figure 3. Laser Raman spectra of (a) poly(PyPDO)-600, (b) poly(PyPDO)-700, and (c) poly(PyPDO)-800.

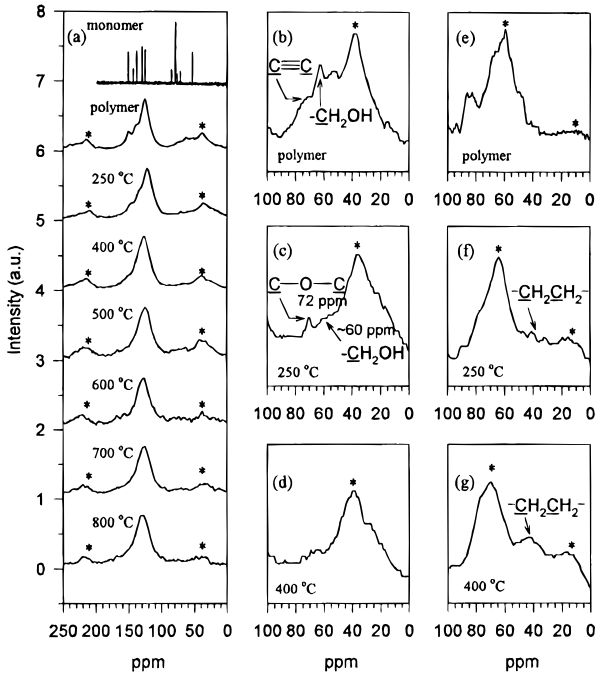

Figure 4. ^{13}C NMR spectra of monomer, poly(PyPDO), and poly(PyPDO)-T_p; the spectra of all the samples except monomer are investigated by CP/MAS technique (the spinning rate is 6500 Hz for a−d and 4500 Hz for e−g).

disordered graphite-like structures.[18] The former corresponds to A_{1g} vibration mode which becomes Raman active because of the finite size of the graphite crystallites. The latter is due to structural defects of the graphite crystal. The peak at ~1350 cm^{-1} indicates that these specimens contain small crystallites of graphite. If the sample has the exact graphite structure, the spectrum should show only a single first-order line at ~1580 cm^{-1} due to E_{2g} vibration mode of the graphite lattice.[19]

Additional information about the structures of poly(PyPDO) and poly(PyPDO)-T_p (T_p: 250 and 400 °C) was obtained from ^{13}C NMR spectra as shown in Figure 4. Because of the insolubility of the metathesis polymer and pyropolymers, the spectra are obtained by the CP/MAS method except for the monomer. The asterisk marked on top of the peak denotes the spinning side bands of the peak at ~125 ppm caused by the high-speed rotation.[20] In the ^{13}C NMR spectrum of PyPDO, the peaks in the region 120−150 ppm correspond to pyridyl sp^2 carbons (Figure 4a). These peaks are broadened and merged into a single peak near 110−170 ppm (Figure 4b) upon polymerization.[21] The peaks of the monomer near 69−83 ppm corresponding to sp carbons also turned into a single broad peak as shown in Figure 4b. The sp and sp^3 carbon peaks of the poly(PyPDO), however, are observed near 70 and 60 ppm, respectively. The downfield shift of the sp^3 carbons is due to the deshielding of those carbons by polymer backbone. In the spectrum of poly(PyPDO)-250 (Figure 4c), the peaks near 50−80 ppm have almost disappeared, suggesting that aromatization has proceeded simultaneously with the dehydration of the pendant groups to give the ether and methylene groups. In the spectrum of poly(PyPDO)-250, however, the resonance peaks corresponding to the unreacted hydroxymethyl carbons are still detected near 60 ppm. When the temperature is raised to 400 °C, the peaks of the ether and hydroxymethyl carbons almost disappeared (Figure 4d). All the pyropolymers produced under 600 °C show enhanced intensity for the side band near 37.6 ppm due to methylene groups produced by dehydration. The peak area of the side bands near 37.6 and 211.5 ppm become about the same only over 600 °C. The integration value of the 37.6 ppm peak is almost twice that of the 211.5 ppm peak, indicating that there are other peaks below the side band near 37.6 ppm and that a methylene linkage exists in the poly(PyPDO)-T_p (T_p < 600 °C). The change in the integration values is shown in Table 3. The methylene carbon peaks, however, can be clearly detected under the lower spinning rate conditions (Figure 4e,f). When the sample is heat-treated at over 400 °C, the peak near 150−170 ppm decreased and the shape of the sp^2 peaks sharpened, suggesting that the pyridinic carbons have changed into a different form (Figure 4a).

Table 3. Integration Ratio of Main Peak and Side Bands in ^{13}C NMR CP/MAS Spectra[a]

materials	37.6 ppm	125 ppm
poly(PyPDO)	1.1	4.1
poly(PyPDO)-250	1.5	4.6
poly(PyPDO)-400	1.6	4.5
poly(PyPDO)-500	1.6	4.0
poly(PyPDO)-600	1.3	4.2
poly(PyPDO)-700	1.0	4.4
poly(PyPDO)-800	0.9	4.4

[a] The peak area at 37.6 and 125 ppm is divided by that of 211.5 ppm to estimate the relative integration ratio from Figure 4a. The area between 50 and 80 ppm is not estimated.

The XPS spectra of poly(PyPDO) and its pyropolymers are shown in Figures 5 and 6. Because the monomer

(18) Yudasaka, M.; Kikuchi, R.; Matsui, T.; Ohki, Y.; Yoshimura, S.; Ota, E. *Appl. Phys. Lett.* **1994**, *65*, 46.
(19) Tuinstra, F.; Koenig, J. L. *J. Chem. Phys.* **1970**, *53*, 1126.
(20) Akhter, M. S.; Chughtai, A. R.; Smith, D. M. *Carbon* **1985**, *23*, 593.
(21) Yamabe, T.; Yamanaka, S.; Tanaka, K.; Terao, T.; Maeda, S.; Yata, S. *Phys. Rev.* **1988**, *37*, 5808.

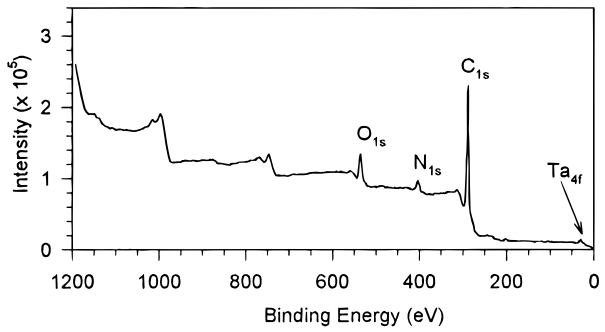

Figure 5. XPS spectra of poly(PyPDO); wide-scan spectrum.

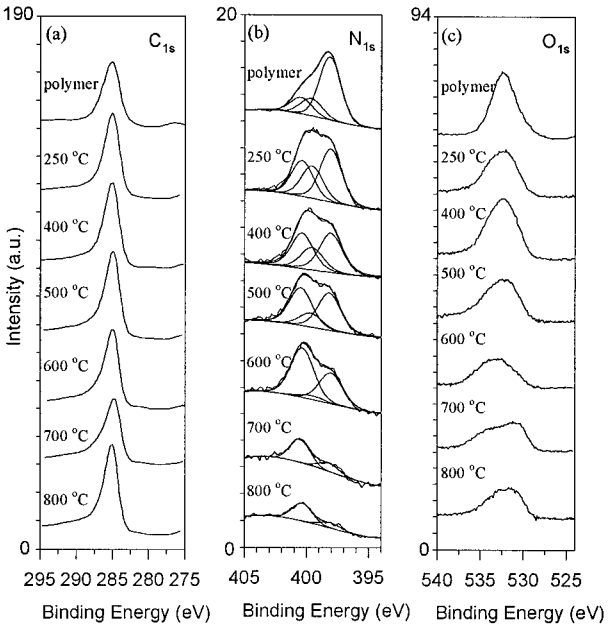

Figure 6. XPS spectra of poly(PyPDO)-T_p; (a) C_{1s}, (b) N_{1s}, and (c) O_{1s} level.

has an alcoholic moiety, metal alkoxide could be generated during polymerization (metal from catalysts used). According to the XPS results (Figure 5), however, the content of Ta is very small. The atomic percent of each atom is as follows: C_{1s} (82.3%), O_{1s} (10.6%), N_{1s} (6.7%), Ta_{4f} (0.5%). The peaks arising from the C_{1s} level are corrected to 285 eV because of charging effects, and the shakeup satellite bands are detected near 290−292 eV. Generally, the shakeup satellite bands are observed at lower kinetic energy region by ~7 eV, indicating the presence of aromatic structures in polymers.[22] Peak tailing is observed in the higher binding energy region suggesting that there are oxygen and nitrogen in these pyropolymers (Figure 6a). The shape of peaks in the region of the N_{1s} level is varied and broadened upon heat treatment at various temperatures.[22] Pels et al. reported four distinct N_{1s} peaks in the XPS spectra of carbonaceous materials: pyridinic nitrogen (398.6 ± 0.3 eV), pyrrolic nitrogen (400.5 ± 0.3 eV), quaternary nitrogen (401.3 ± 0.3 eV), and the *N*-oxide of pyridinic nitrogen (402−405 eV).[23] Poly(PyPDO)-T_p (T_p > 400 °C) shows also peaks corresponding to quaternary nitrogens near 401.5 eV and the intensity of these peaks gradually

(22) Briggs, D.; Seah, M. P. *Practical Surface Analysis*; John Wiley and Sons: New York, 1990.

(23) Pels, J. R.; Kapteijn, F.; Moulijn, J. A.; Zhu, Q.; Thomas, K. M. *Carbon* **1995**, *33*, 1641.

Table 4. Deconvoluted Results of N_{1s} Level of XPS Spectra[a]

materials	pyridinic N	pyrrolic N	pyridinium N
poly(PyPDO)	65.8	17.9	16.8
poly(PyPDO)-250	44.2	26.8	29.9
poly(PyPDO)-400	41.2	23.9	37.4
poly(PyPDO)-500	42.7	15.8	43.4
poly(PyPDO)-600	37.0	4.5	59.7
poly(PyPDO)-700	27.6	1.5	76.4
poly(PyPDO)-800	22.3	0.1	79.6

[a] All the data are given as the percent value; the measured N_{1s} levels were analyzed using the nonlinear least-squares minimization routine after cubic polynomial background subtraction. The fitted components were deconvoluted by using Gaussian and Lorentzian functions.

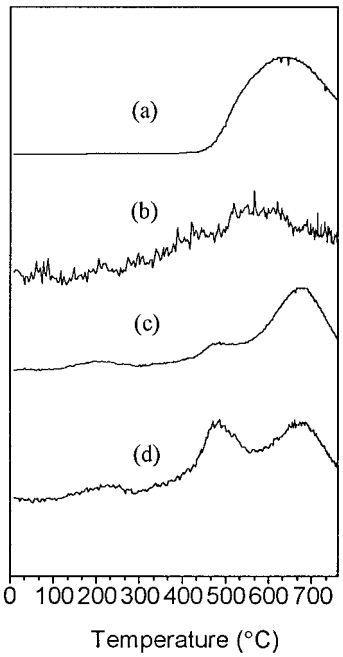

Figure 7. Temperature-programmed desorption profiles of (a) H_2, (b) H_2O, (c) HCN, and (d) CN.

increased compared to other components, especially the pyridinic-N component (Figure 6b and Table 4), on heat treatment.

The reason the polymer has a quaternary nitrogen is presumably due to some pyridyl moieties changing their form to a salt type with HCl during the quenching of the polymerization. In the case of the pyropolymers (T_p > 400 °C); however, the counteranion corresponding to the quaternary nitrogens can be hydroxide or cyanide ions evolved during the pyrolysis as shown in Pels's report.[23] The peaks of the O_{1s} level becomes broader upon heat treatment due to oxidation of carbon or nitrogen functionalities as was mentioned previously (Figure 6c).[15,22]

The temperature-programmed desorption (TPD) experiments (Figure 7) show that evolution of hydrogen molecules from poly(PyPDO) increases sharply over 500 °C (Figure 7a) in contrast to the EA study which indicated a continuous decrease of hydrogen upon heat treatment. These are attributed to spontaneous transfer of hydrogen atoms from hydrogen sources (e.g., −OH, $-CH_2-$, −CH=CH−, etc.) to give different fragments under 500 °C. The exact evaluation of all of these secondary fragments is very difficult under the severe pyrolysis conditions. The peak at m/e = 18 corresponding to H_2O continuously increased from room temper-

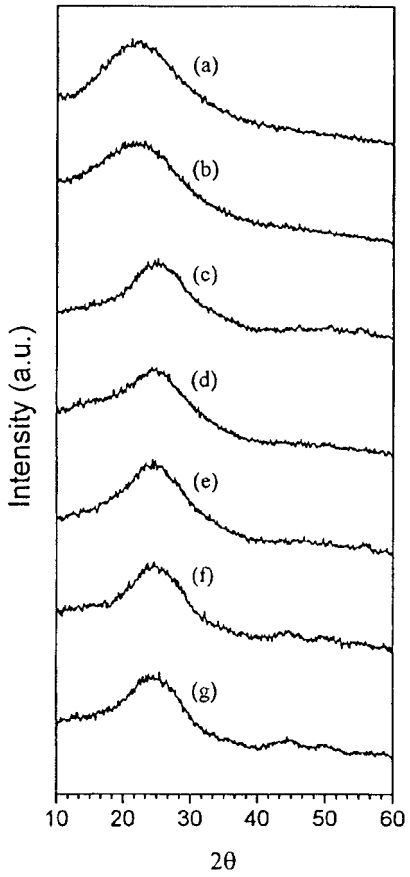

Figure 8. X-ray diffraction patterns of (a) poly(PyPDO), (b) poly(PyPDO)-250, (c) poly(PyPDO)-400, (d) poly(PyPDO)-500, (e) poly(PyPDO)-600, (f) poly(PyPDO)-700, and (g) poly(PyPDO)-800.

ature to 600 °C (Figure 7b). The reason why dehydration from the hydroxymethyl pendant group is not observed is presumably due to trapping of the water generated into the micropores of these polymers to give other forms of oxygen functionalities by oxidation processes. The fragments having *m*/*e* of 27 and 26 are observed over 400 °C (Figure 7c,d), and the pattern of these two fragments is very similar to each other, suggesting that these fragments are HCN and CN. The difference of intensity near 700 °C in these fragmentation profiles is due to the change of HCN into H_2. In addition to these fragmentations, changes in the peak at 28 (*m*/*e*) are observed, suggesting that N_2 or ethylene gas is also evolved during pyrolysis.

To check the stacking parameter of the pyropolymers, a powder X-ray diffraction analysis was carried out on heat treated poly(PyPDO) as shown in Figure 8. In poly(PyPDO) and heat-treated poly(PyPDO), all the peaks are broad, indicating that these samples do not show ordered stacking. As T_p was raised, however, the pyropolymers were gradually arranged to give a plate structure having shorter interlayer distance than those prepared at low temperature, although the whole structure is still disordered. A significant phase change was observed at around 400 °C due to the condensation of the pyridyl rings from the polymer side chains to give a more planar structure. When poly(PyPDO) was pyrolyzed at 700 °C for 30 min, peaks are generated at around 40−55°. The XRD spectrum of poly(PyPDO)-800 shows three broad peaks at 2θ of around 25, 44, and 53°. According to the standard X-ray diffraction

Table 5. Charge/Discharge Capacity and Cyclic Efficiency of Poly(MPBEY)-750, Poly(DPBEY)-750, and Poly(PyPDO)-800[a]

	capacity (mAh/g)					efficiency (%)	
	discharge		charge		irreversible capacity[b]		
materials	1st	2nd	1st	2nd	(mAh/g)	1st	2nd
poly(MPBEY)-750[c]	882	283	324	231	558	37	82
poly(DPBEY)-750[d]	713	302	275	260	438	39	86
poly(PyPDO)-800[d]	822	339	353	296	469	43	87

[a] Electrolytes used in the test: 1.0 M $LiPF_6$/EC+DMC (2:1). Abbreviation: EC (ethylene carbonate); DMC (dimethyl carbonate). [b] Irreversible capacity in the first cycle. [c] The electrode test was carried out by using a two-electrode cell. [d] Three-electrode system.

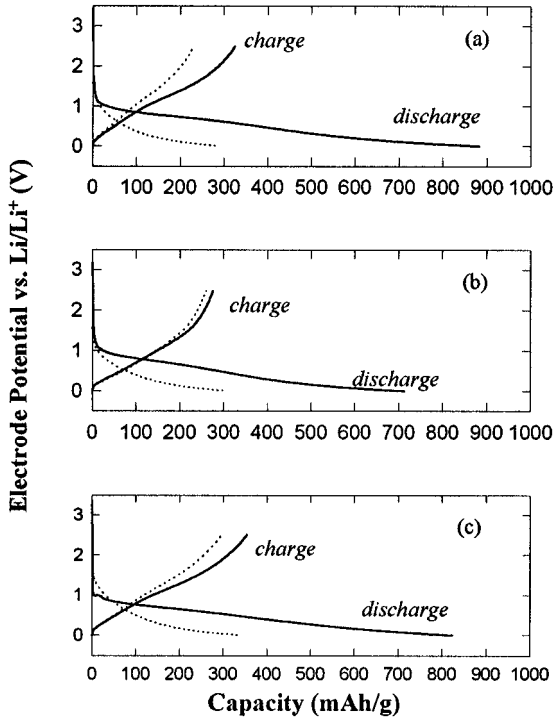

Figure 9. Charge/discharge curves of (a) poly(MPBEY)-750, (b) poly(DPBEY)-750, and (c) poly(PyPDO)-800; the solid and dot lines corresponds to first and second cycles, respectively.

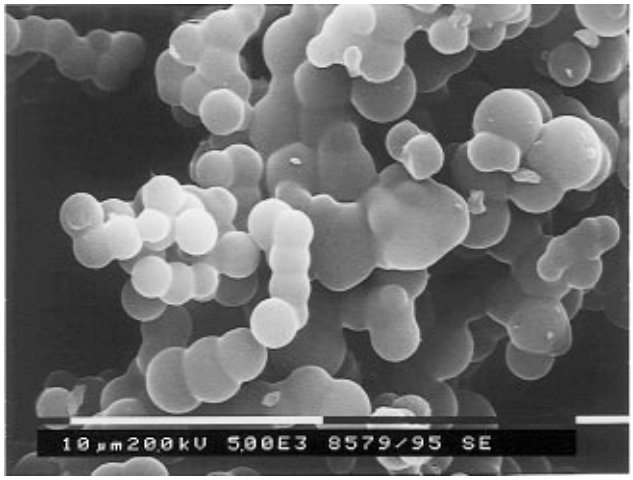

Figure 10. SEM photograph of the poly(PyPDO)-800. The length of white solid line drawn in the picture is 10 μm.

patterns of natural graphite, the peaks at 2θ of 20−30° is assigned to the (002) band, at 42−48° to the (100) and (101) bands and the additional band near 53° to the (004) band, respectively. From the half-widths of

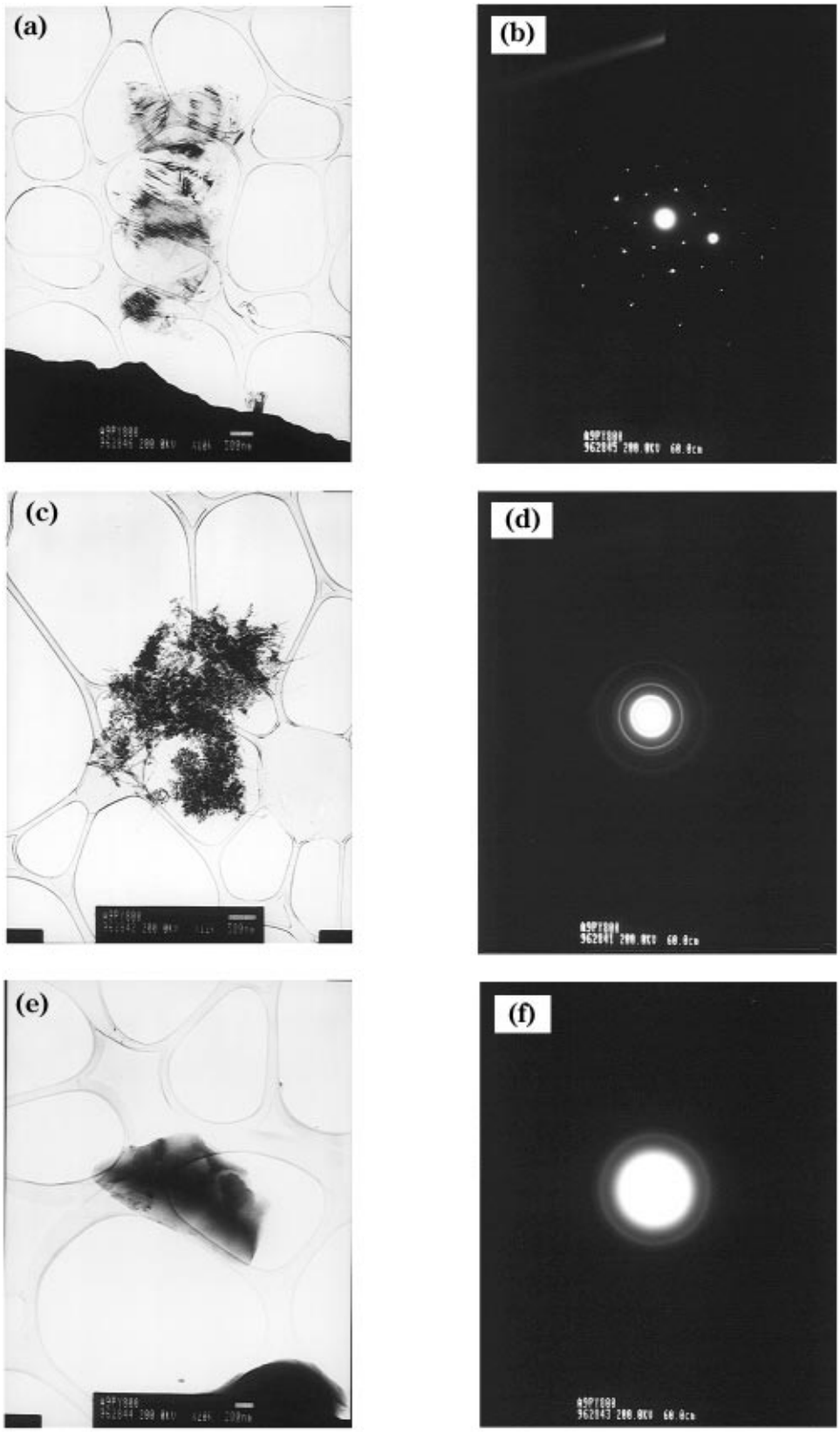

Figure 11. TEM photographs of poly(PyPDO)-800; (a) graphitic particle, (c) aggregation of ordered particles having small graphitic domain, (e) disordered particle; (b), (d), and (f) are the electron diffraction patterns of (a), (c), and (e), respectively.

the (100) bands, the lateral extent of the graphene sheets (L_a) of poly(PyPDO)-800 is estimated to be about 28.0 Å.[24,25] Because the intensity of the (101) band at 42.4° is 5 times higher than that of the (100) band at 44.6°, these bands are not easily isolated in the case of poly(PyPDO)-T_p (T_p: 700 and 800 °C). Thus, the L_a value is estimated after the fitting of the XRD curve. These XRD patterns are very similar to those of poly-

(24) Dahn, J. R.; Sleigh, A. K.; Shi, H.; Reimers, J. N.; Zhong, Q.; Way, B. M. *Electrochim. Acta* **1993**, *38*, 1179.

(25) *JCPDS*; International Center for Diffraction Data: 1601 Park Lane, Swarthmore, PA, 1980; pp 22−1069.

[(*Z*)-1-methoxy-4-phenyl-1-buten-3-yne]-750 [poly(MPBEY)-750] and poly(1,4-diphenyl-1-buten-3-yne)-750 [poly(DPBEY)-750],[10,11] which show high-capacity Li insertion/deinsertion properties as shown in Table 5. The results suggest poly(PyPDO)-T_p ($T_p \geq 700$ °C) to have Li insertion/deinsertion properties like poly(MPBEY)-750 and poly(DPBEY)-750.

Figure 9 shows the charge/discharge curves of the specimens in Table 5. The charge/discharge curves for poly(PyPDO)-800 (Figure 9c) are very similar to those of pyropolymers which do not have nitrogens. Dahn et al. proposed that nitrogen affects the electrochemical behavior of lithium ion in two ways.[12] First, the irreversible capacity observed in the first cycle increases with the nitrogen content of samples. Second, the incorporated nitrogen causes a shift of the cell capacity to lower voltages compared to pure carbon electrodes. Regardless of the differences in the composition, all the samples tested show a large hysteresis in the second cycle. Also, the staging phenomena which takes place in graphites are not observed even though the majority of the lithium is inserted near 0 V, suggesting that the nitrogen in poly(PyPDO)-800 has no effect on the Li insertion properties. The lithium insertion/deinsertion properties of poly(PyPDO)-800 containing nitrogen show large differences from those of Dahn's work. Detailed studies of the Li insertion (discharge)/deinsertion (charge) mechanism are in progress.

The SEM (scanning electron microscopy) image of a poly(PyPDO)-800 particle reveals that it has a beadlike structure as shown in Figure 10. This image is very different from that of poly(MPBEY)-800 reported by Suh and Shim.[10] Poly(PyPDO)-800 has a beadlike structure with micropores of various size, rendering interesting electrochemical properties.

TEM (transmission electron microscopy) images of the poly(PyPDO)-800 particles show that poly(PyPDO)-800 is a mixture of graphitic and carbonaceous materials. The quantity and size of the crystalline particles increased with elevating T_p. Figure 11a shows a photograph of a graphitic particle from the poly(PyPDO)-800 sample. This particle shows the morphology of a single crystal of graphite, and this is verified in the selected area electron diffraction (SAD) pattern as shown in Figure 11b. Figure 11c shows another particle which has a somewhat disordered morphology unlike that of the particle shown in Figure 11a. The crystallinity of this particle, however, is also very high. The SAD pattern of this particle suggests that many graphitic domains aggregate with one other. The particles shown in Figure 11e are disordered particles which do not have an ordered stacking of graphene sheets. The SAD pattern of these particles is shown in Figure 11f.

Summary

5-(2-Pyridyl)-2,4-pentadiyn-1-ol (PyPDO) was polymerized to give poly(PyPDO) by metathesis polymerization over $NbCl_5$- or $TaCl_5$-based catalysts. This precursor polymer was easily converted into polyacene-based or graphite-like pyropolymers containing nitrogen and oxygen on vacuum pyrolysis. The results of elemental analysis, TGA, FT-IR, laser Raman, NMR, XPS, X-ray diffraction, temperature-programmed desorption experiments, SEM, and TEM studies show that major nitrogen functionalities incorporated into graphene layers of the pyropolymers are quaternary nitrogen in the polymers pyrolyzed under severe conditions (e.g., >700 °C). Oxygen is eliminated continuously as small volatile molecules such as water from these pyropolymers. The charge/discharge curves for poly(PyPDO)-800 are very similar to those of pyropolymers which do not have nitrogens.

Acknowledgment. This investigation was supported by the Organic Chemistry Research Center—Korea Science and Engineering Foundation and the Korea Advanced Institute of Science and Technology. The authors are grateful to Mr. Yongju Jung for helpful discussions on the electrochemical analysis and to Mr. Chang Hyun Ko for the TPD experiment and to Mr. Jeong Won Kim for the deconvolution of the XPS spectra.

CM960283N